Supporting Information

Antifouling Coatings of Catecholamine Copolymers on Stainless Steel

Li Qun Xu[1], Dicky Pranantyo[1], Ying Xian Ng[2], Serena Lay-Ming Teo[2*], Koon-Gee Neoh[1], En-Tang Kang[1*], Guo Dong Fu[3]

[1] Department of Chemical & Biomolecular Engineering
National University of Singapore
Kent Ridge, Singapore 117576

[2] Tropical Marine Science Institute
National University of Singapore
Kent Ridge, Singapore 119223

[3] School of Chemistry and Chemical Engineering
Southeast University
Jiangning District, Nanjing, Jiangsu Province, P.R. China 211189

* To whom correspondence should be addressed:
E-mails: cheket@nus.edu.sg (ETK); tmsteolm@nus.edu.sg (SLMT)

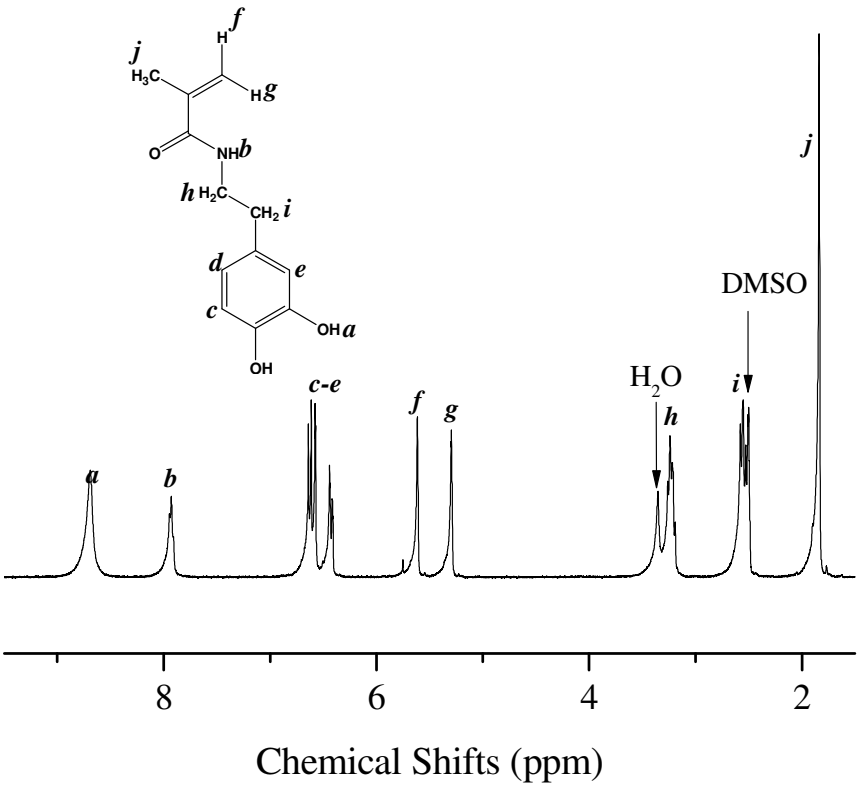

Figure S1. ^{1}H NMR spectrum of DMA in DMSO-d_6.

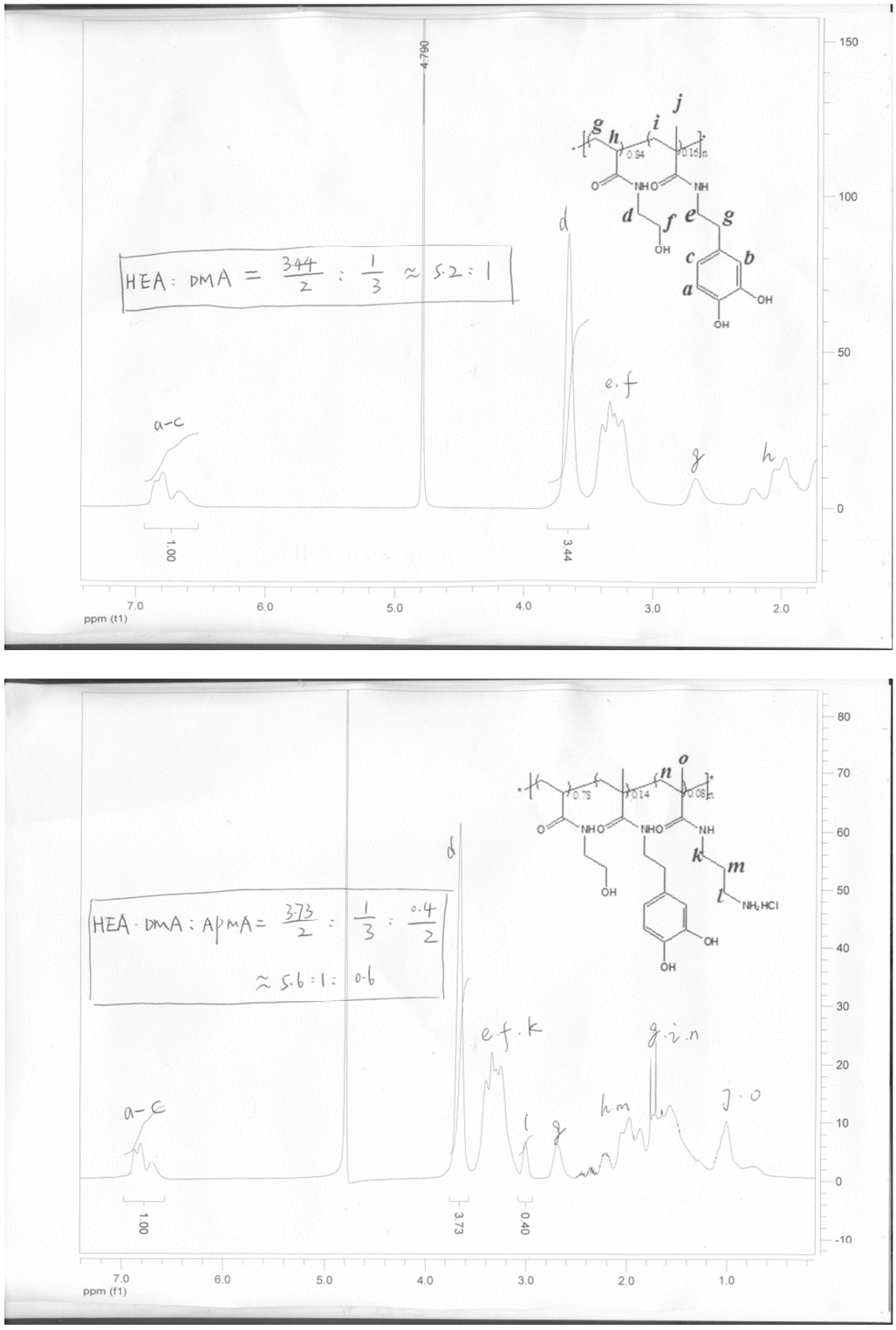

Figure S2. ^{1}H NMR spectra of the P(HEA-*co*-DMA) copolymers and the P(HEA-*co*-DMA-*co*-APMA) terpolymers in D_2O.

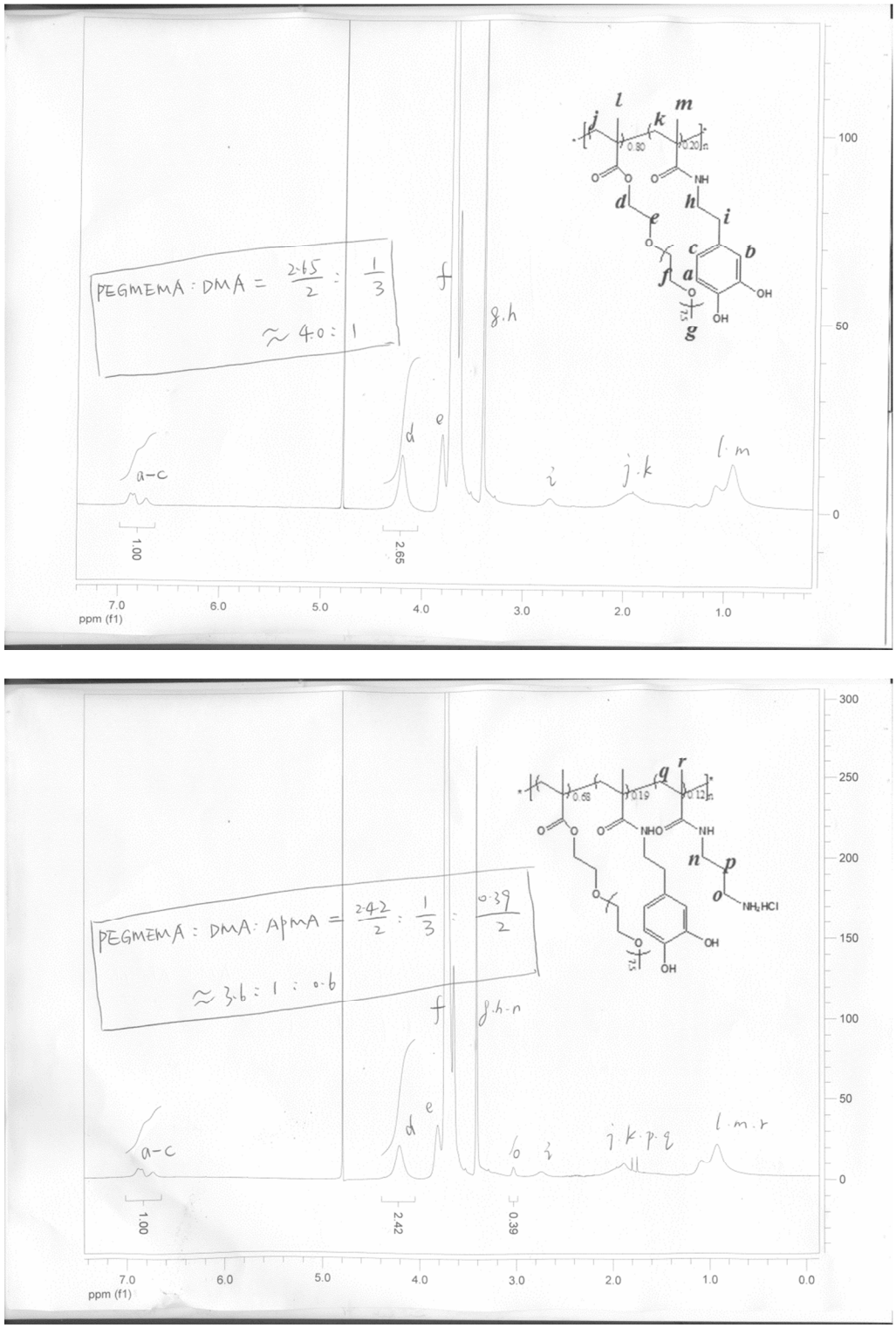

Figure S3. ^{1}H NMR spectra of the P(PEGMEMA-*co*-DMA) copolymers and the P(PEGMEMA-*co*-DMA-*co*-APMA) terpolymers in D_2O.

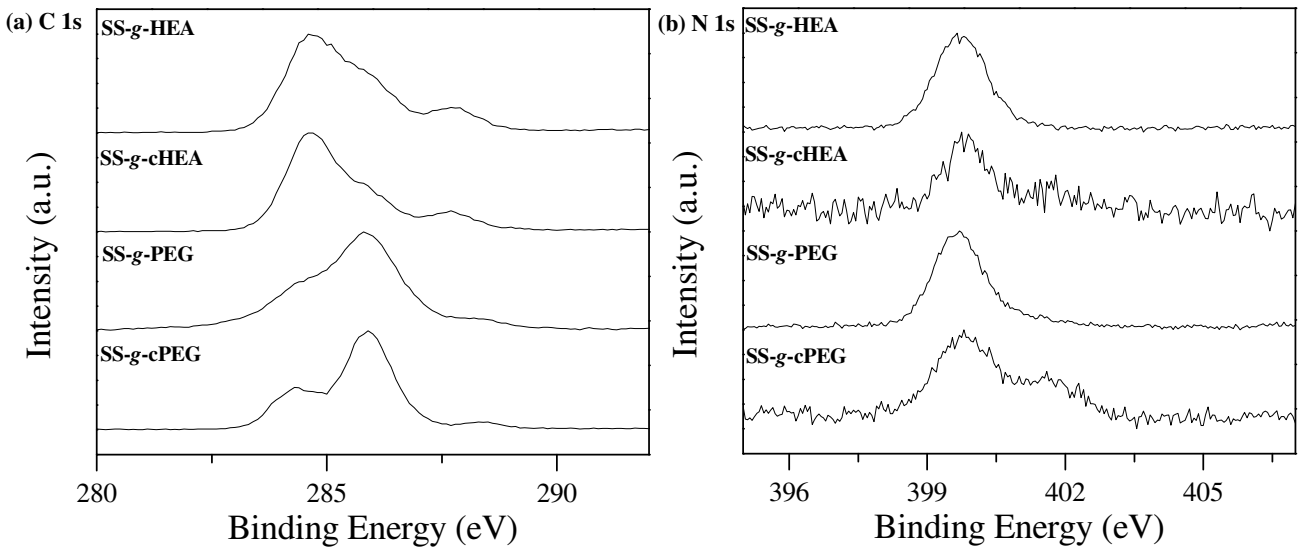

Figure S4. XPS (a) C 1s and (b) N 1s core-level spectra of the P(HEA-*co*-DMA) and P(PEGMEMA-*co*-DMA) copolymers- and the P(HEA-*co*-DMA-*co*-APMA) and P(PEGMEMA-*co*-DMA-*co*-APMA) terpolymers-coated SS surfaces.

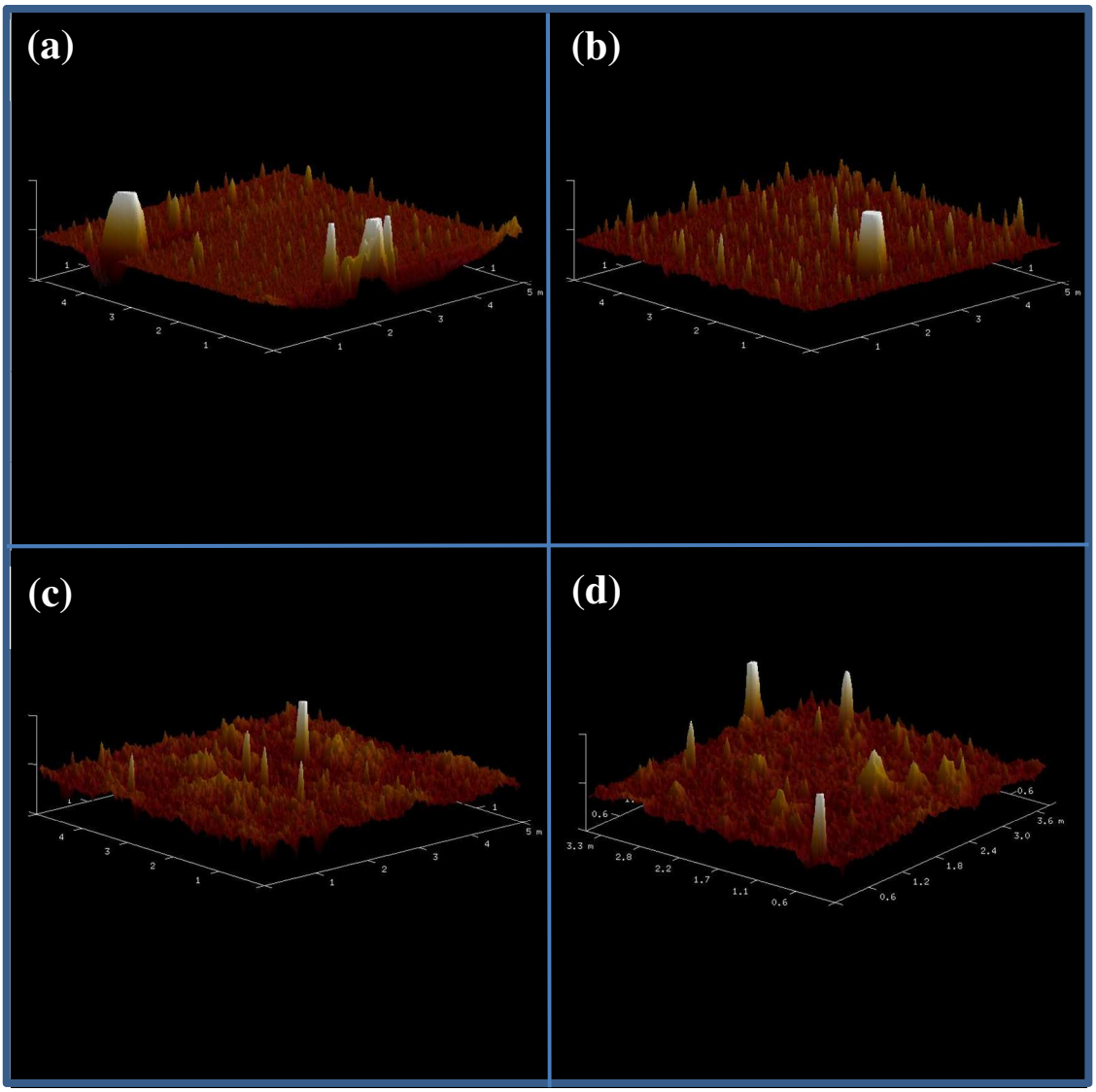

Figure S5. AFM images of the surface of the (a) P(HEA-*co*-DMA) and (b) P(PEGMEMA-*co*-DMA) copolymers- and the (c) P(HEA-*co*-DMA-*co*-APMA) and (d) P(PEGMEMA-*co*-DMA-*co*-APMA) terpolymers-coated quartz slides.

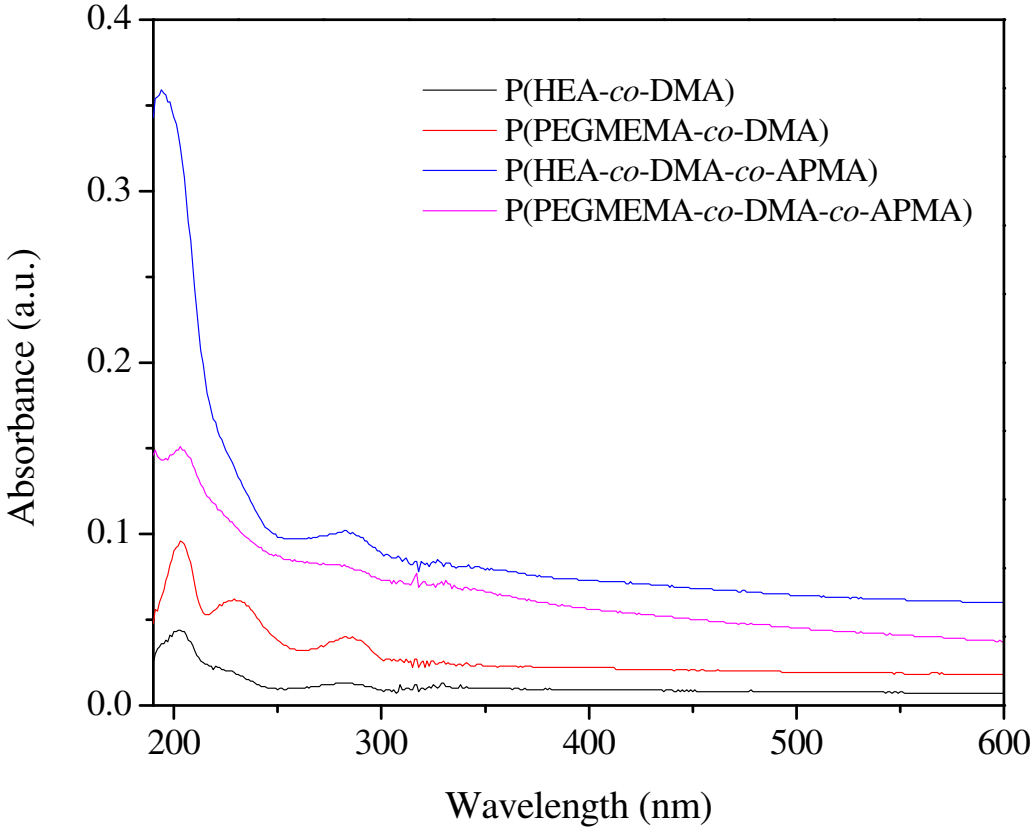

Figure S6. UV-Visible absorption spectra of the P(HEA-*co*-DMA) and P(PEGMEMA-*co*-DMA) copolymers- and the P(HEA-*co*-DMA-*co*-APMA) and P(PEGMEMA-*co*-DMA-*co*-APMA) terpolymers-coated quartz slides.

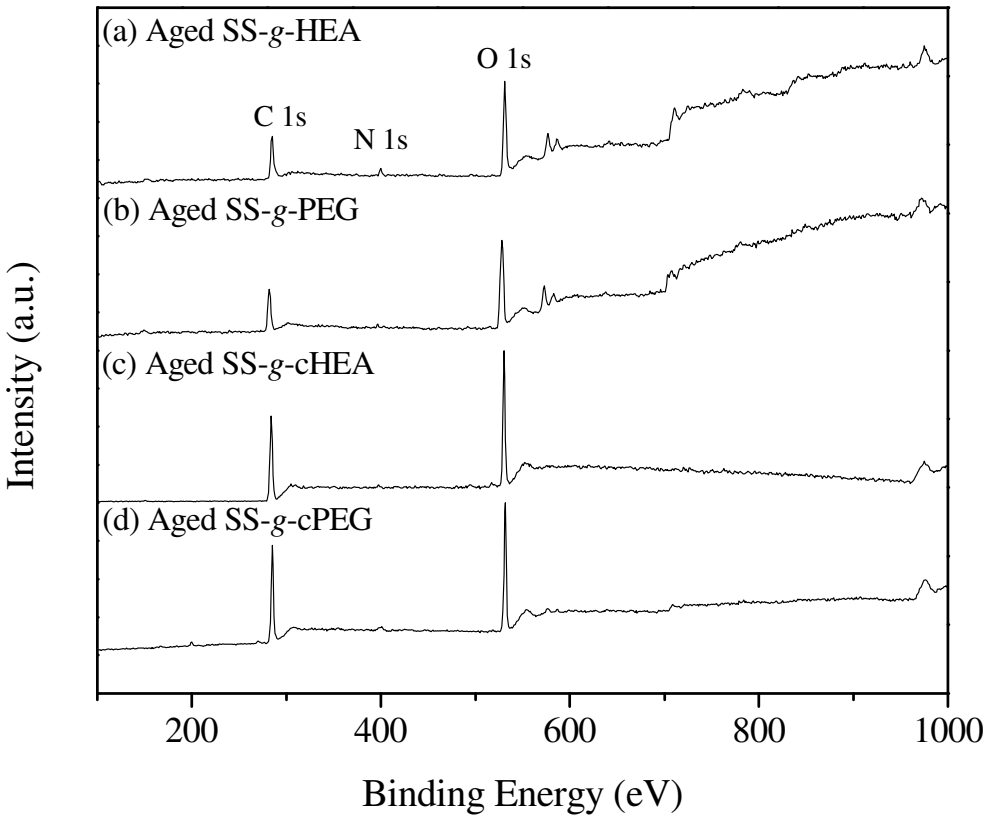

Figure S7. XPS wide-scan spectra of the aged (a) SS-*g*-HEA, (b) SS-*g*-PEG, (c) SS-*g*-cHEA and (d) SS-*g*-cPEG surfaces after exposure to the continuous stream of artificial seawater for 14 days. (The spectra are normalized to the maximum peak intensity.)

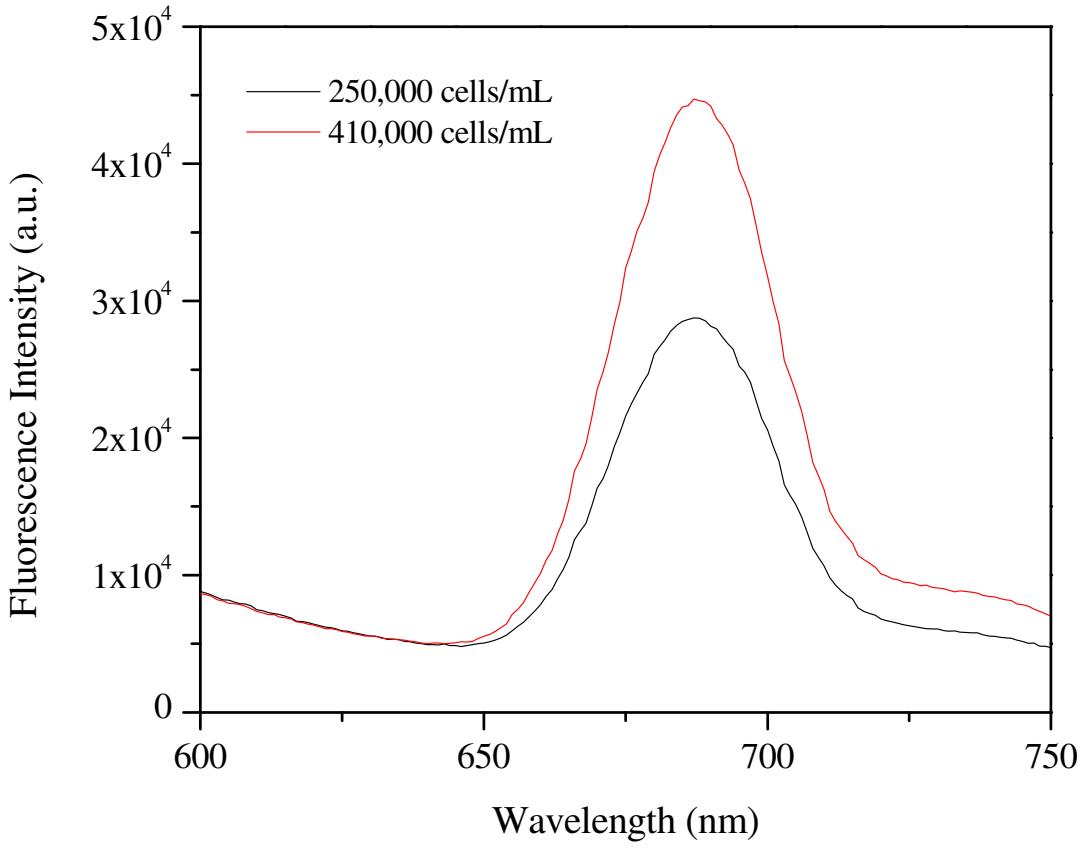

Figure S8. Fluorescence emission spectra of *Amphora* cells at an excitation wavelength (λ_{ex}) of 440 nm. Since the *Amphora* cells exhibit a major emission peak centered at about 690 nm at an excitation wavelength (λ_{ex}) of 440 nm, attributed to the autofluorescence of chlorophyll, the fluorescence technique can be employed to measure the concentration of ultrasonically removed *Amphora* cells.

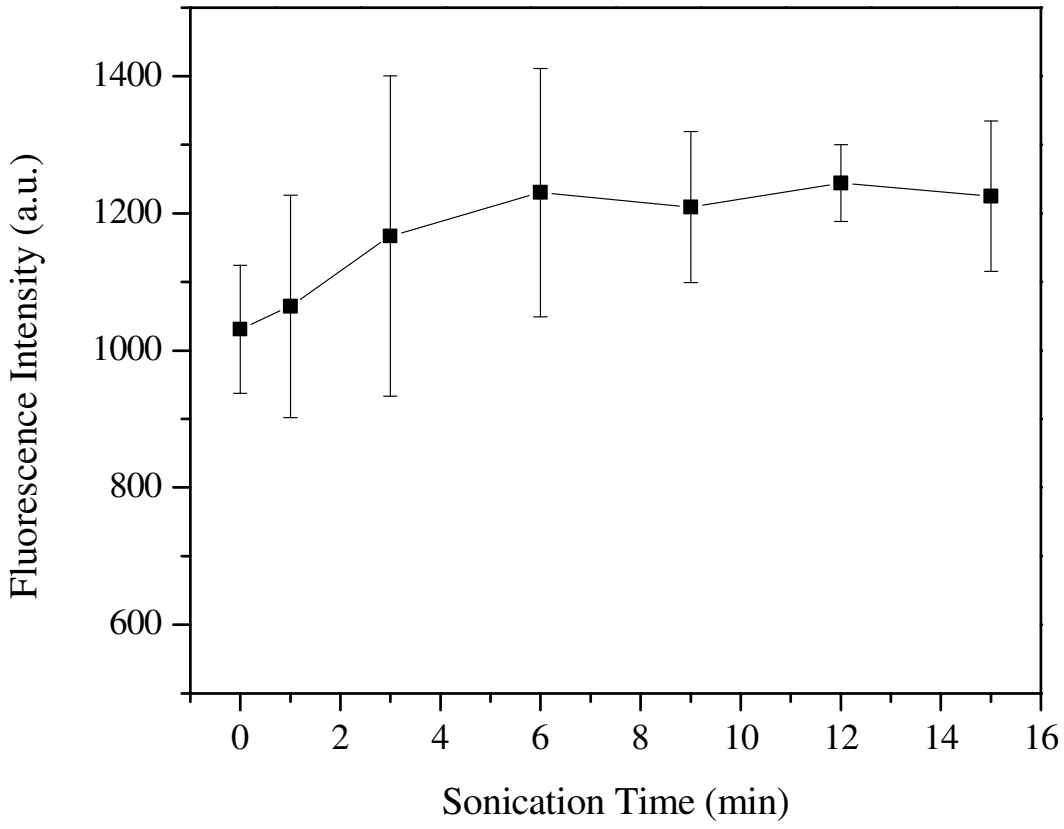

Figure S9. The evolution of fluorescence intensity of *Amphora* cells at 690 nm as a function of sonication time. The fluorescence intensity of *Amphora* cells increases slightly (~18%) with the increase in sonication time and reaches a plateau after about 6 min, suggesting that the ultrasonic treatment has only limited effect on the fluorescence intensity of *Amphora* cells. The enhancement in fluorescence intensity is probably due to better dispersion of the *Amphora* cells upon ultrasonic treatment.

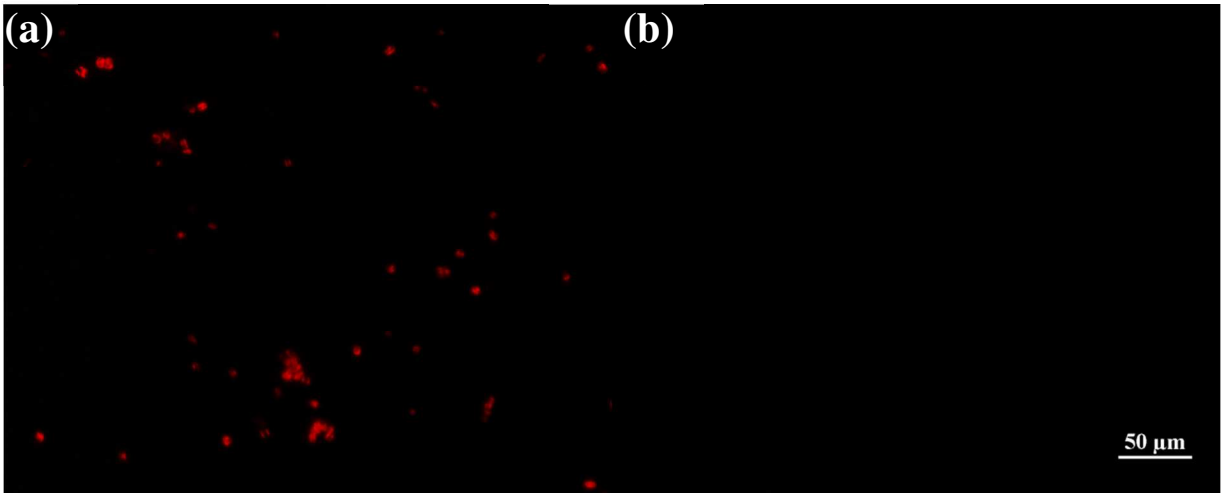

Figure S10. Fluorescence images of *Amphora* cells on pristine SS surfaces (a) before and (b) after ultrasonic treatment. The adherent *Amphora* cells on the substrates were viewed with a Nikon Eclipse Ti microscope, equipped with an excitation filter of 535 nm and an emission filter of 617 nm. A large numbers of *Amphora* cells were observed on the pristine SS surface, while almost no *Amphora* cell was visible on the surface after sonication for 10 min. This result confirms that the *Amphora* cells on the SS surface can be effectively dislodged by sonication.

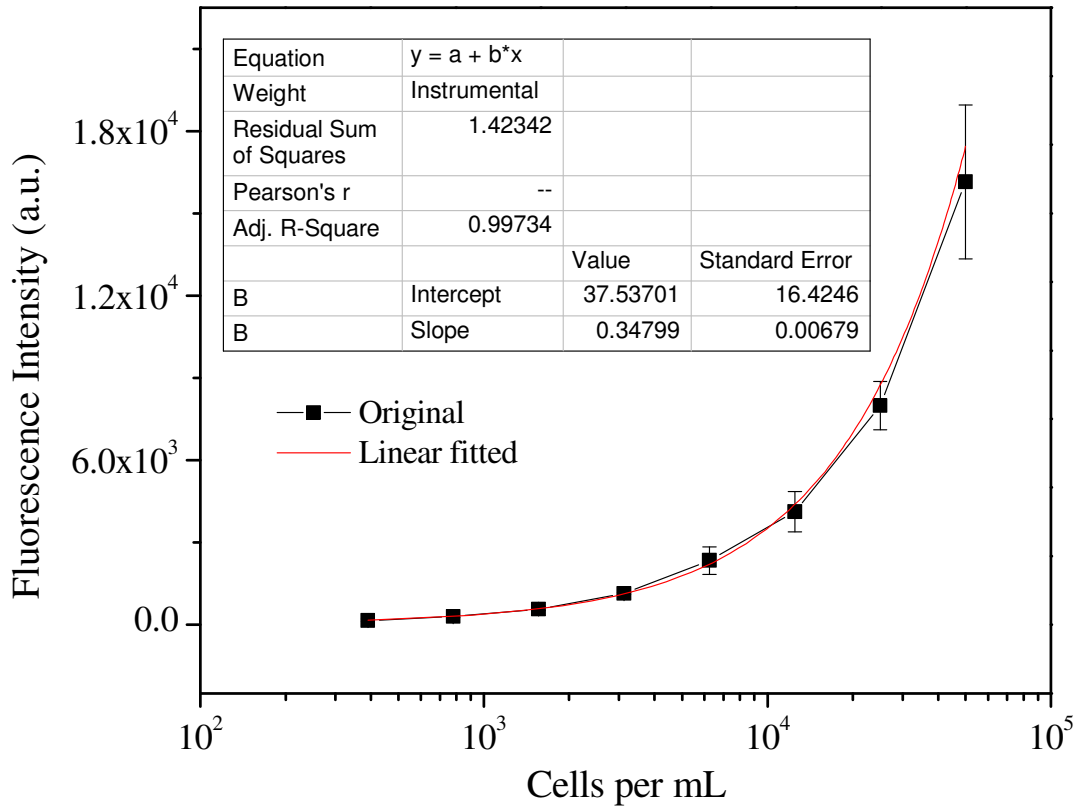

Figure S11. The plot and fitted curve of the number of *Amphora* cells versus the fluorescence intensity of the cells at 690 nm.